



NEW ZEALAND SOCIETY FOR EARTHQUAKE ENGINEERING

2019 Pacific Conference on Earthquake Engineering

TURNING HAZARD AWARENESS INTO RISK MITIGATION

4 – 6 April | SkyCity, Auckland | New Zealand



Methodology for soil compliant inelastic spectrum & some observations

R.D. Jury

Beca, Wellington.

A.J. Carr

University of Canterbury, Christchurch

Carr Research Ltd., Christchurch,

MC Consulting Engineers, Christchurch

A.M. Puthanpurayil

Beca, Wellington.

ABSTRACT

Conventionally a constant ductility inelastic spectrum is computed using a fixed base single degree of freedom (SDOF) system. Although this might be acceptable for a system which has minimum soil flexibility, it might not be acceptable for a system where soil flexibility might be expected to influence the building response. A methodology is illustrated in this paper whereby an inelastic spectrum with constant ductility incorporating soil flexibility can be computed. The soil flexibility is introduced using a simplified soil spring model. In this preliminary study the soil stiffness is linearized using an equivalent linearization procedure and the structure inelasticity is represented using a “*Bilinear hysteresis*”. A comparison is made between the modified inelastic spectrum obtained and the classical inelastic spectrum relying on fixed base SDOF system. It is shown that incorporation of soil flexibility does effect the inelastic spectrum and is very important when an inelastic spectrum is used to justify the design adequacy of a structural system. Some preliminary results on the effect of choice of hysteresis on basin effects are also presented. From the results it can be observed that the “peaks” in the elastic spectrum not disappear completely by using a high ductility system.

1 INTRODUCTION

An inelastic spectrum is the inelastic counterpart of the elastic spectrum. Structures subjected to severe earthquakes exhibit inelastic deformations. An inelastic spectrum provides a direct method to evaluate these effects rather than relying on the pseudo conventional approach of reducing the elastic spectral ordinates by constant factor based on equal energy or equal displacement assumptions.

2 MOTIVATION FOR THE PRESENT STUDY

Normally an inelastic spectrum is generated using an effective single degree of freedom system with fixed boundary conditions. In other words, the classical methodology does not account for the effect of soil (Carr 2012). This initial paper forms a part of a larger research effort initiated to investigate the basin effects on design spectra. The authors believe that a framework that considers soil compliance is very important when investigating basin effects on design spectra. Nonlinear behaviour softens a structure so that it could potentially move into a period range of higher response as the effect of soil flexibility could lead to resonance amplifications in several cases. In this paper, a novel method for generation of inelastic spectra incorporating soil compliance is discussed. It has been shown in the paper that soil compliance does influence the generated inelastic spectrum. As the focus of this paper is to present the framework and illustrate the effects, only arbitrary soil parameters are used in the example. More research needs to be done with varying soil parameters to completely unravel the effects.

Most of the commercial packages that generate inelastic spectra only attribute elasto-plastic hysteresis to the superstructure and use a fixed boundary condition. As a first attempt, a set of results is also presented showing the effects of choice of different hysteresis on the generated inelastic spectrum. To be consistent with the computer programs available commercially, only fixed base boundary conditions are presented in this study. Along with elasto-plastic hysteresis, three additional hysteresis models have been used to generate inelastic spectra for the example ground motion. It is shown that the choice of hysteresis is of utmost importance when evaluating the dissipation generated by an inelastic spectrum even with fixed boundary conditions. It has been shown that both the level of ductility and choice of hysteresis influences these “peaks” in the spectrum.

Albeit, this paper only presents some preliminary results, these give a clear indication that further research is needed to fully understand these effects. Also incorporating the soil compliance in generating the inelastic spectrum is essential if realistic conditions are to be reflected in the generated spectrum.

3 INELASTIC SPECTRA GENERATION

A very brief outline of the method used for the spectra generation used in the present study is described here.

- I. For an assumed structural mass, define the range of structural period and the incremental period.
- II. Perform an elastic time history analysis for the selected period and find the elastic strength corresponding to the selected period.
- III. Iterate the yield strength as a fraction of the elastic strength and compute the system ductility. If the system ductility matches the target ductility then the responses are recorded and forms part of the inelastic spectrum. If it does not match the iteration is continued till convergence is obtained.

4 SOIL COMPLIANCE ENHANCED SDOF SYSTEM

This section develops the framework for generating the an inelastic spectrum for a flexible based system.

Figure 1 shows a soil enhanced multi-degree of freedom with inelastic super-structure and elastic soil medium. A reduced order soil model with discrete equivalent translational and rocking springs are used in the present study (Gazetas G 1991).

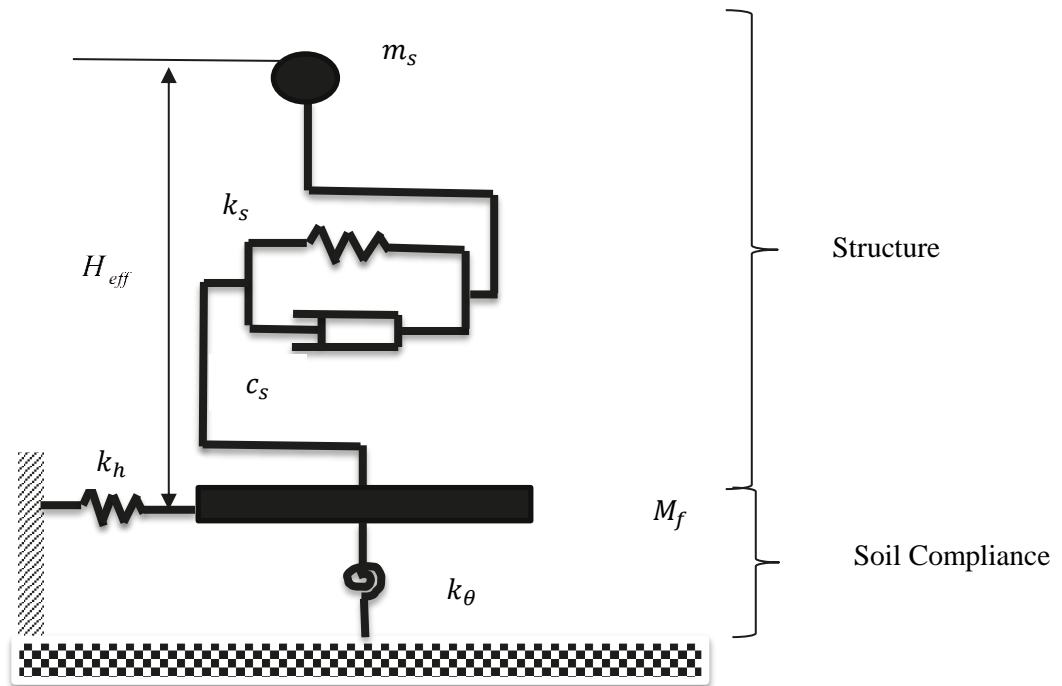


Figure 1: Soil Compliance Enhanced SDOF System

Ignoring the degree of freedom at the foundation slab level (Akehashi et al. 2018) as shown in Figure 2 and assuming the static series spring we get,

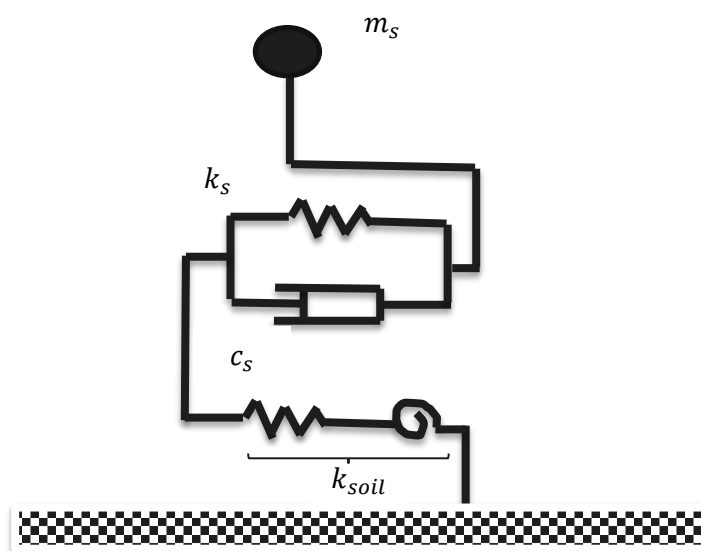


Figure 2: Soil Compliance Enhanced SDOF System

$$\frac{1}{k_{soil}} = \frac{1}{k_h} + \frac{H_{eff}^2}{k_\theta} \quad (1)$$

Here,

$$\left. \begin{aligned} k_h &= \alpha_x K_x \\ K_x &= \frac{8}{2-\vartheta} Gr_x \\ r_x &= \sqrt{\frac{A_f}{\pi}} \\ k_\theta &= \alpha_\theta K_\theta \\ K_\theta &= \frac{8}{3(1-\vartheta)} Gr_\theta^3 \\ r_\theta &= \sqrt[4]{\frac{4I_f}{\pi}} \\ a_0 &= \omega r / v_s \end{aligned} \right\} \quad (2)$$

where G is the soil dynamic shear modulus, A_f is the area of the foundation, I_f is the moment of inertia of the foundation, ω is the angular frequency, r is r_x for translational deformation modes and r_θ for rotational deformation modes, v_s is the soil shear wave velocity and ϑ is the soil Poisson ratio. α_x and α_θ are approximated from Figure 3. In the Figure 3, β_s refers to the hysteretic damping ratio.

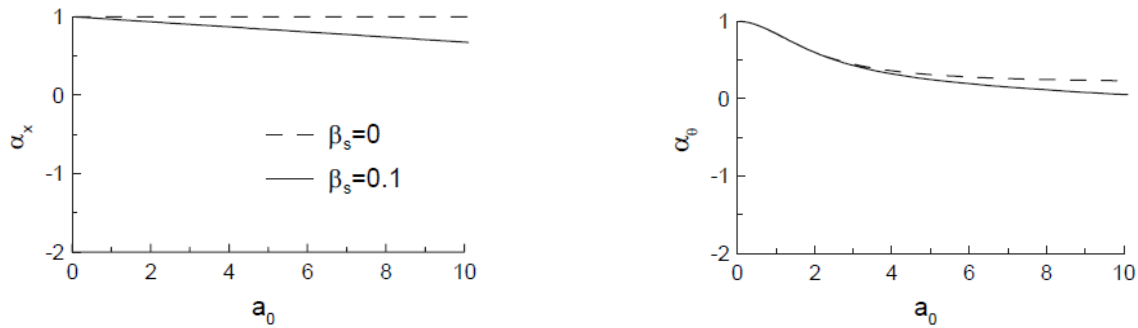


Figure 3: Foundation Stiffness Factors for Elastic and Visco-elastic Halfspaces ($\vartheta = 0.4$) (FEMA 440; Veletsos & Verbic, 1973)

Assuming,

$$\beta = \frac{k_s}{k_{soil}} \quad (3)$$

$$k_{soil} = \frac{k_s}{\beta} \quad (4)$$

As shown in figure 4,

$$K_{eff} = \frac{k_s k_{soil}}{k_s + k_{soil}} \quad (5)$$

Substituting Equation (4) in Equation (5) we get,

$$K_{eff} = \frac{k_s}{\beta + 1} \quad (6)$$

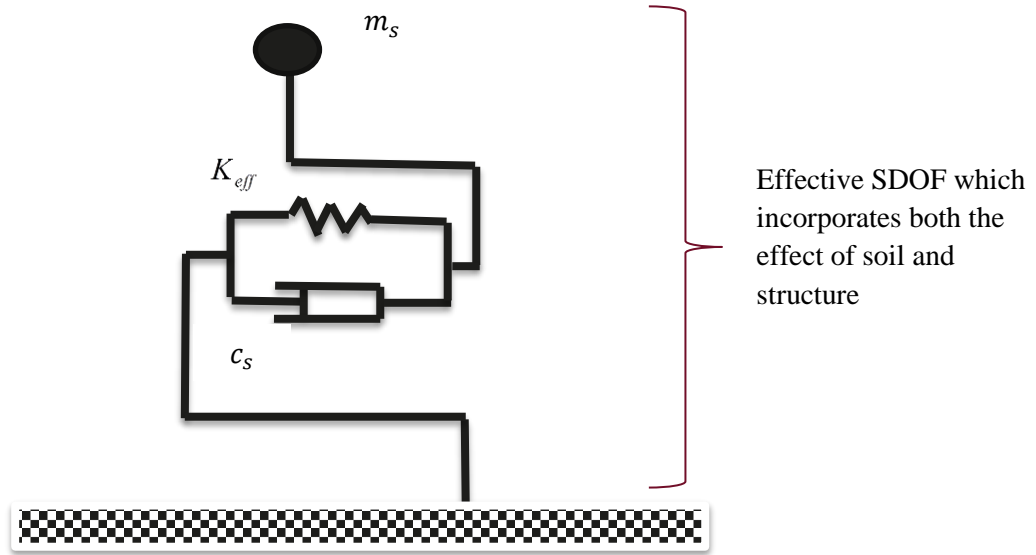


Figure 4 Soil Compliance Enhanced Effective SDOF System

Now converting to an effective SDOF system as represented by Figure 4.0, we get,

$$\tilde{M}\ddot{x}(t) + \tilde{C}\dot{x}(t) + k_s(t)x(t) = -M1\ddot{x}_g(t) \quad (7)$$

Here,

$$\left. \begin{aligned} \gamma &= \frac{k_s}{K_{eff}} = \beta + 1 \\ \tilde{M} &= \gamma m_s = (\beta + 1)m_s \\ \tilde{C} &= \gamma c_s = (\beta + 1)c_s \end{aligned} \right\} \quad (8)$$

Substituting Equation (8) into Equation (7) we get,

$$(\beta + 1)m_s\ddot{x}(t) + (\beta + 1)c_s\dot{x}(t) + k_s(t)x(t) = -m_s\ddot{x}_g(t) \quad (9)$$

Equation (9) represents the equation of motion with damping represented by a viscous model. It can be solved incrementally using Constant Average Newmark total equilibrium framework with structural stiffness following any known hysteresis pattern (Carr 2012). The inelastic spectra may be generated using the steps described in Section 3.0.

In the same framework other damping models may also be incorporated with slight modification.

Incorporating a time hysteresis damping model Equation (9) is modified as follows,

$$(\beta + 1)m_s\ddot{x}(t) + (\beta + 1) \int_0^t g(t - \tau) \dot{x}(\tau) d\tau + k_s(t)x(t) = -m_s\ddot{x}_g(t) \quad (10)$$

Here $g(t - \tau)$ is a causal damping kernel function and represents a non-viscous damping phenomenon because integration by parts of the model would result in a displacement dependent damping model.

Equation (10) is an integro-differential equation and maybe solved using the AAR method (Puthanpurayil et al. 2014; Puthanpurayil et al. 2018). In the present study no further investigation has been carried out on this aspect.

5 NUMERICAL ILLUSTRATION

The earthquake acceleration strong motion record obtained during the 2016 Kaikoura event at the BNZ Wellington location has been used in the present study for generating the inelastic spectra. This site is located within Wellington basin.

5.1 Flexible inelastic spectra

Equation (9) is solved using the classical Newmark equilibrium method and adopting the steps described in Section 2.0, the flexible based inelastic spectrum is generated. Figure 5 depicts the flexible inelastic spectrum. It should be noted that in order to generate the flexible base spectrum the soil parameters need to be chosen. In a realistic scenario this can be determined for the specific site under consideration. As the sole intention of this paper is to illustrate the methodology, qualitative realistic values for soil parameters have been adopted as per Gazetas (1991). To provide a datum the fixed base inelastic spectrum is also plotted in Figure 5. It can be clearly seen that flexible base spectrum is different from the fixed base inelastic spectrum. It is expected the effects of soil compliance will become more prominent on soft soils. This inelastic spectrum adopts a bilinear hysteresis for the super structure.

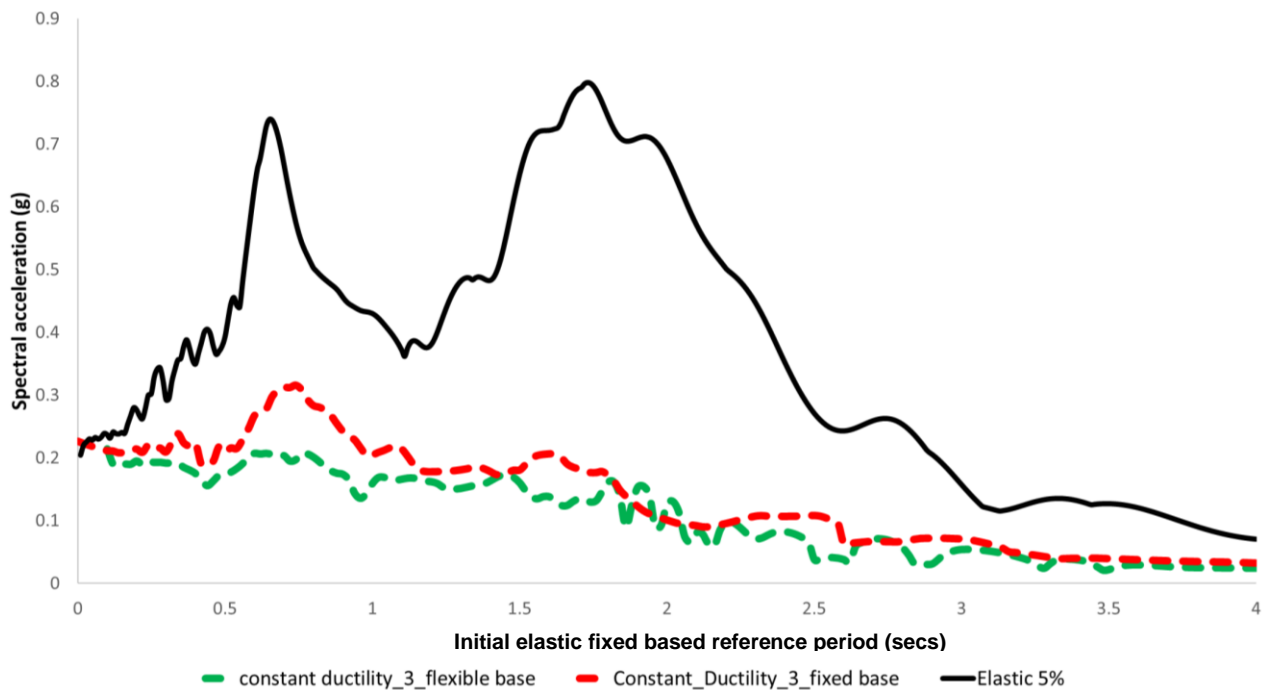


Figure 5: Flexible Base Inelastic Spectrum

It must be noted that effect of soil compliance is sensitive to the choice of the soil parameters. For the specific choice of soil parameters made for this study it can be seen that inclusion of soil compliance generally reduces the spectral amplitude; *but it must be noted that this is not expected to be the case for all scenarios*. More research effort need to be expended to reach a more robust conclusion on this aspect.

5.2 Some observations on basin edge effects based on fixed base inelastic spectra

In this section a preliminary study is presented on the basin effects and the effect of different hysteresis choice on the observed “peaks” in the long period range of the elastic spectrum. Figures 6 to 9 represent the effect of different hysteresis on the peaks in the elastic spectra.

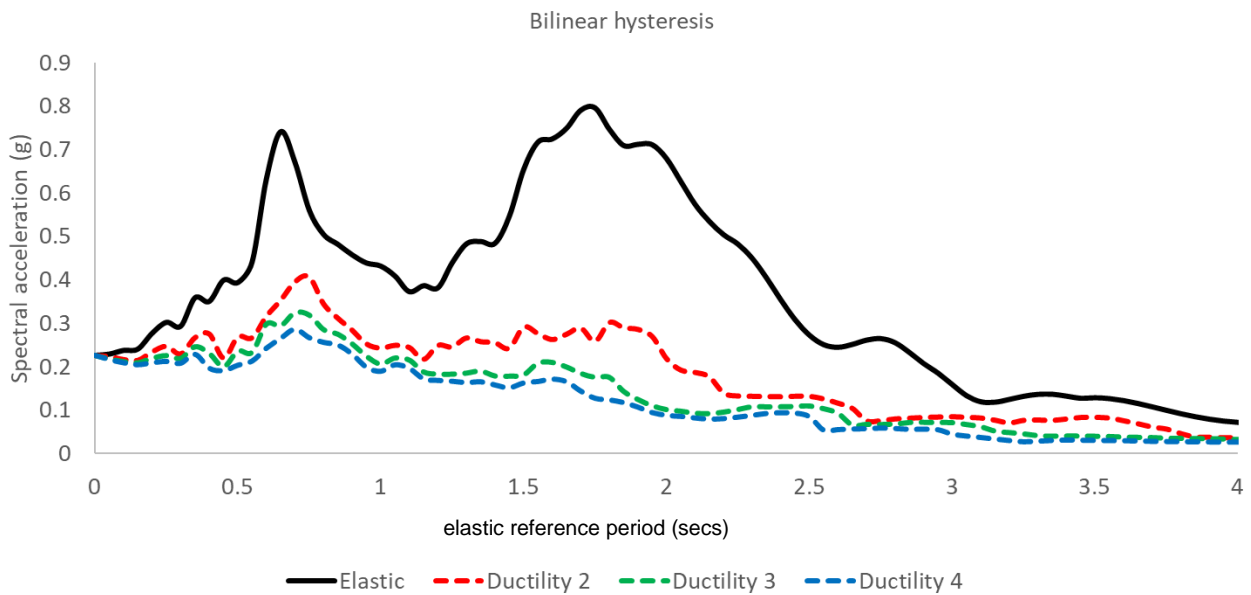


Figure 6: Inelastic Spectra :Bilinear Hysteresis

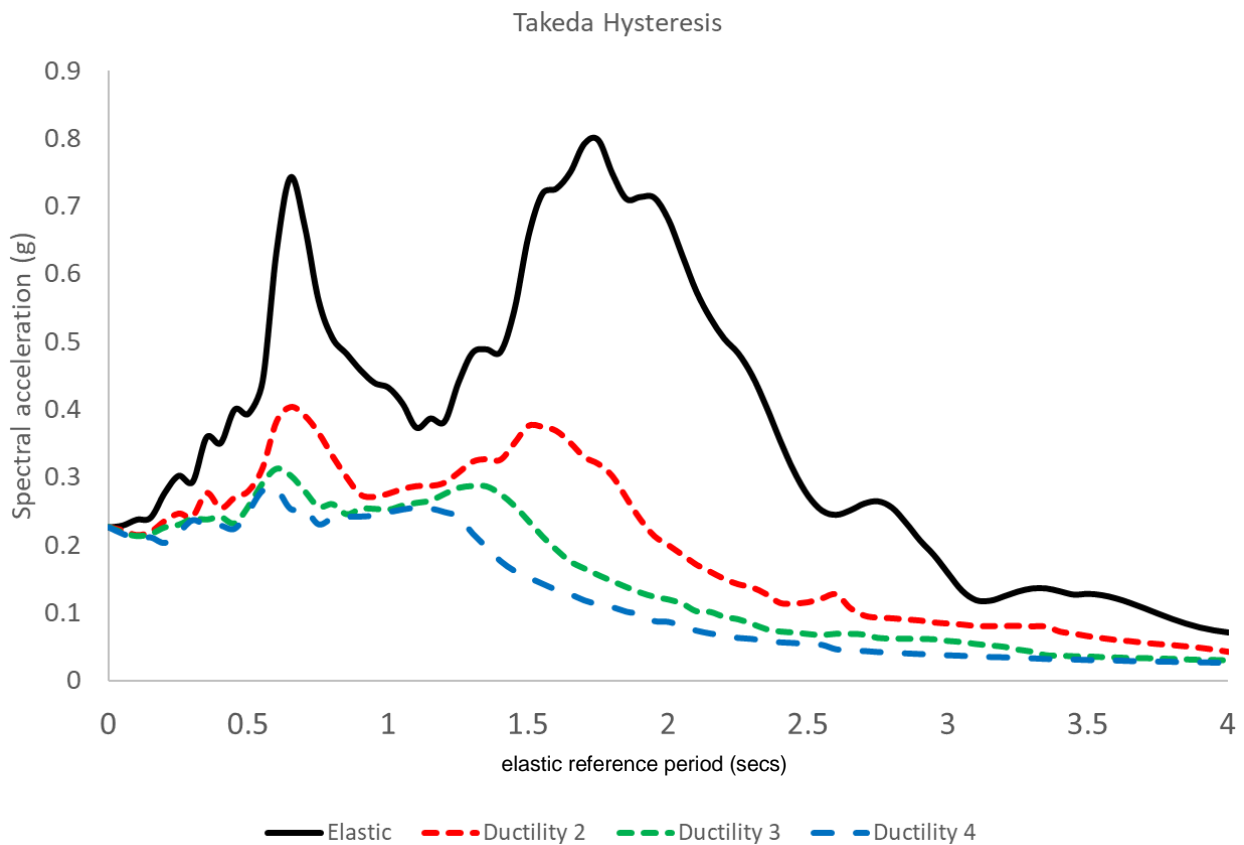


Figure 7: Inelastic Spectra: Takeda Hysteresis

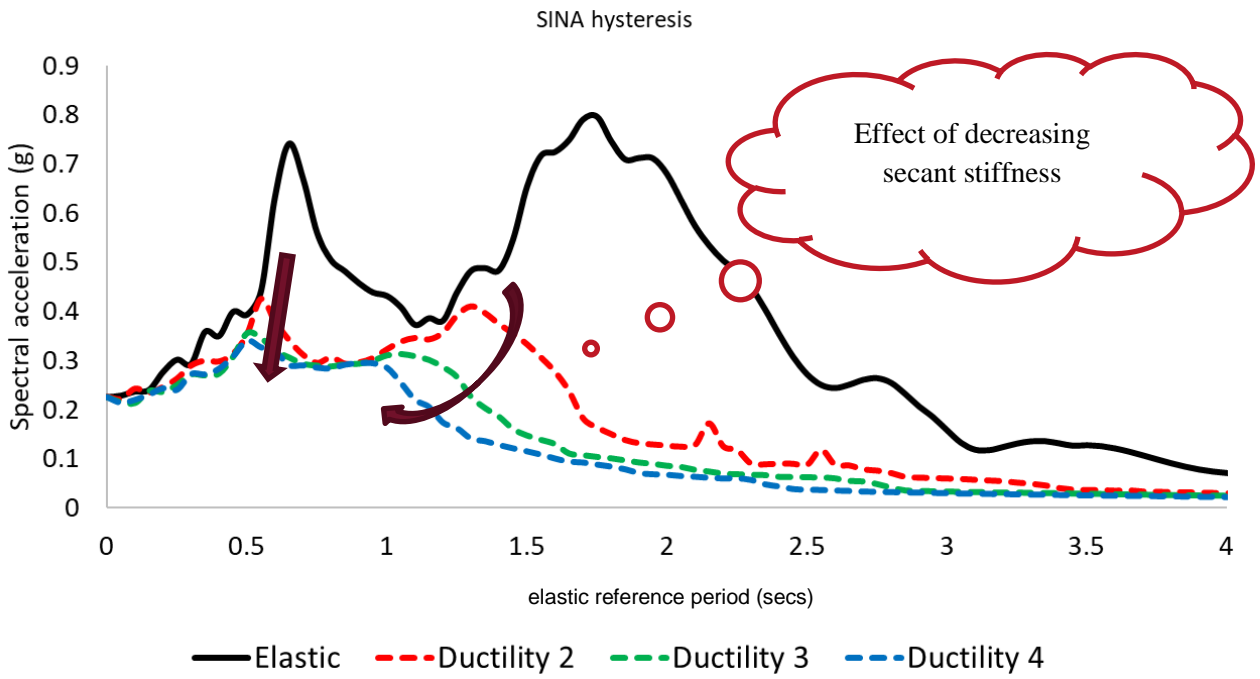


Figure 8: Inelastic Spectra: SINA Hysteresis

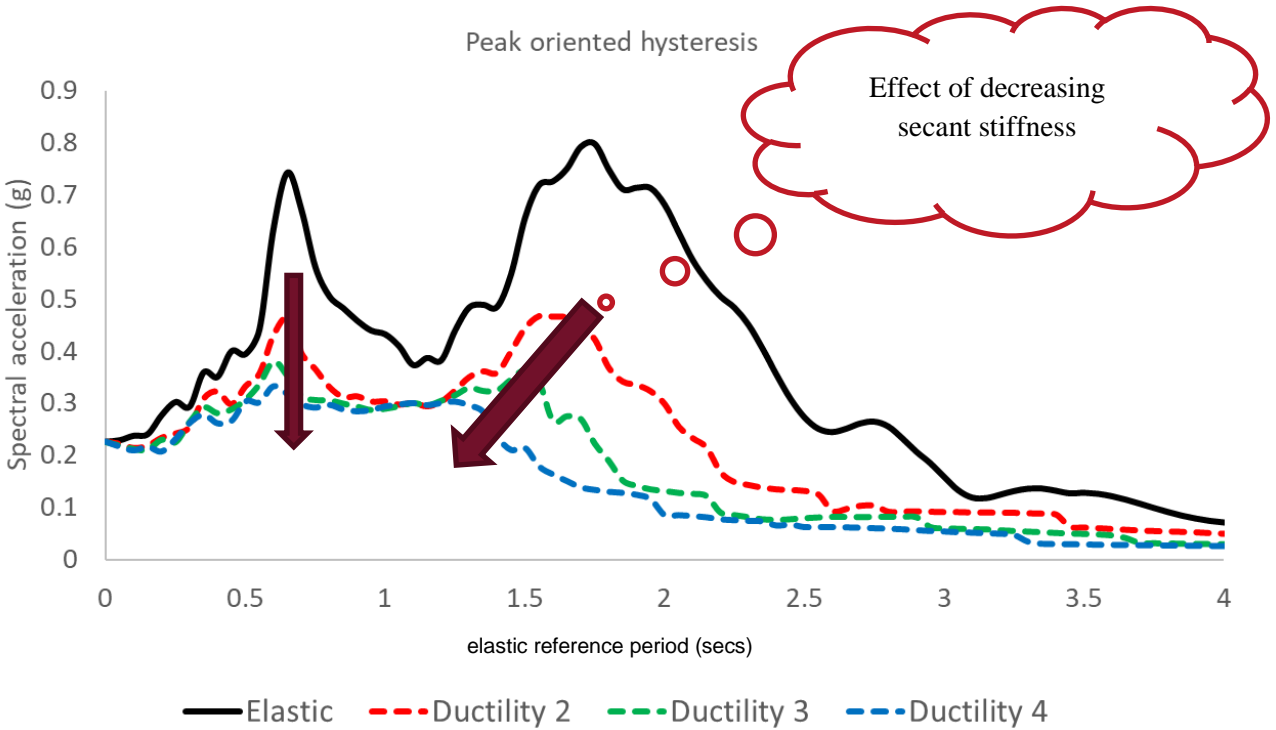


Figure 9: Inelastic Spectra: Peak-Oriented Hysteresis

It can be clearly seen from these plots that the different hysteresses exhibit different effects on the observed peaks. The bilinear hysteresis, which is a highly idealised simplified version of hysteresis exhibits the largest

level of dissipation as the level of ductility increases whereas the peak-oriented hysteresis exhibits a lower level of dissipation. This is a very important observation mainly because in reality none of our structures exhibit a bilinear or close to elasto-plastic response. In other words, the disappearance of peaks exhibited by elasto-plastic inelastic spectra as the level of ductility increases may not be a reality. An effective shifting of the peak is observed in all the spectra. But it must be noted that period to which the peak ordinate of the spectrum is plotted is not the effective secant period of the system, but the initial elastic period of the system. It is possible that the level of reduction of the “peaks” is an effect associated with energy dissipation in the hysteretic system and by the shift in effective natural period shown by the hysteretic system. The longer period “peaks” do diminish with increasing energy dissipation and does provide a degree of protection for base-isolated structures subject to earthquake ground motions which exhibit these longer period spectral “peaks”. However the elongation of the natural period resulting from the system yield could move the effective natural period towards the period of a “peak” [Andriono 1989]. The base-isolation hysteresis is usually bi-linear like and the elastic spectra “peak” implies greater inelastic demand on the isolation system but does not impose greater accelerations on the structure.

6 CONCLUSIONS AND FUTURE DIRECTIONS

A methodology for generating inelastic spectrum incorporating soil compliance is presented. A preliminary effect of the choice of hysteresis on the inelastic spectrum is illustrated. Based on the study the following conclusions may be drawn:

- The “peaks” exhibited in the elastic spectra do not disappear completely as the level of ductility increases.
- The response characteristics are a function of the choice of hysteresis and the majority of the realistic hysteresis exhibits the fact that “peaks” do not disappear completely as the level of ductility increases.
- The soil compliance has an influence on the generated inelastic spectrum.
- There is an effective period shift exhibited by the “peaks”, but the degree of shifting exhibited might not be the true shift as the peak points are plotted against the initial elastic period as opposed to the effective secant period exhibited by an inelastic system.

7 REFERENCES

- Akehashi, H., Kojima, K., Fujita, K. & Takewaki, I. 2018. *Critical response of nonlinear base -isolated building considering soil-structure interaction under double impulse as substitute for near-fault ground motion*, *Frontiers in Built environment*, DOI: 10.3389/fbuil.2018.00034
- Andriono, T. 1989. *Seismic Resistant Design of Base Isolated Multistorey Structures*. PhD Thesis, Department of Civil Engineering, University of Canterbury.
- Behnamfar, A. 2017.
- Gazetas, G. 1991. Foundation vibrations, Chapter 15, *Foundation Engineering Handbook, 2nd edn* (ed. H.-Y.Fang), Van Nostrand Reinhold, New York, pp. 553–593